

Human [⁷⁴Se]selenomethionine metabolism: a kinetic model^{1,2}

Christine A Swanson, Blossom H Patterson, Orville A Levander, Claude Veillon, Philip R Taylor, Kathy Helzlsouer, Patricia A McAdam, and Loren A Zech

ABSTRACT A study was undertaken to investigate the pharmacokinetics of an organically bound form of selenium. Six adults received a single oral 200- μ g dose of ⁷⁴Se as L-selenomethionine. A kinetic model was developed to simultaneously account for the appearance and disappearance of the tracer in plasma, urine, and feces. The model included absorption distributed along the gastrointestinal tract, uptake by the liver-pancreas subsystem, enterohepatic recirculation, distribution to two large tissue pools, and transport through four components of the plasma pool. Average turnover time of the plasma components varied from 0.01 to 1.1 d. The turnover time in the liver-pancreas subsystem ranged from 1.6 to 3.1 d. Turnover time ranged from 61 to 86 d in the peripheral tissues with the slowest turnover. The whole-body residence time was approximately five-fold greater than the turnover time of the tissue pool with the slowest turnover, reflecting substantial reutilization of labeled material. *Am J Clin Nutr* 1991;54:917-26.

KEY WORDS Selenium, compartmental analysis, pharmacokinetics, stable isotopes, humans

Introduction

Selenium is recognized as a nutrient essential to human health. In parts of China, selenium is administered to selected population groups to prevent a juvenile cardiomyopathy known as Keshan disease (1). Epidemiologic investigations in Finland, a low-selenium area, indicated an association of low selenium status and increased risk of cardiovascular disease (2). In 1984 the amount of selenium in domestic Finnish foods was increased by adding selenium to agricultural fertilizer (3). More recently, some investigators reported an inverse relation of selenium status and cancer risk in both low- and high-selenium areas (4). Controlled clinical trials are in progress to examine the hypothesis that selenium is associated with cancer risk.

Biological activity of selenium is influenced by its metabolic disposition. Selenium metabolism in humans, however, is not well characterized. Estimates of selenium absorption, whole-body retention, and excretion have been obtained from balance and tracer studies. The latter approach more readily exposes the fundamental complexity of selenium utilization. Data from several radio- and stable-isotope studies, for example, indicate that there are multiple metabolic pools of selenium (5-9).

By use of compartmental analysis, an integrated picture of whole-body selenium utilization in humans can be obtained from

kinetic data derived from tracer studies in humans. Patterson et al (10) used this approach to develop a kinetic model for an inorganic form of selenium (sodium selenite), the chemical form of selenium frequently used in animal studies. The predominant form of selenium in food is most likely to be organically bound, primarily in the form of selenomethionine (11). The study reported here was undertaken to develop a kinetic model for an oral dose of an organically bound form of selenium (ie, selenomethionine) and to compare the metabolic parameters of that model with those calculated by using the previously developed selenite model.

Subjects and methods

Subjects and protocol

Six adults recruited from the Beltsville, MD, area participated in a pharmacokinetics study. Characteristics of the subjects, three males and three females, are given in **Table 1**. The study protocol was approved by the National Institutes of Health and US Department of Agriculture Safety and Protocol Monitoring Committees. Subjects signed informed-consent statements and were paid for participation in the study. Participants were required to be in general good health and could not be taking either selenium supplements or other medications. Female subjects could be neither pregnant nor lactating. Screening consisted of a complete medical history, physical examination, and laboratory tests (hematological, biochemical, and urinalysis profiles).

Subjects were fed the same daily diet for 3 d before dose day (day 0) and for 12 d afterward. The study diet furnished, per day, 87 μ g dietary Se, 94 g fat, 304 g carbohydrate, and 98 g protein. Deionized drinking water was provided and energy intake was supplemented with selenium-free lemon-lime soft drinks. All food was prepared at the Beltsville Human Nutrition Research Center. Subjects consumed a self-selected diet before and after the special diet days.

¹ From the National Cancer Institute, National Institutes of Health, Bethesda, MD, and the Beltsville Human Nutrition Research Center, US Department of Agriculture, Beltsville, MD.

² Address reprint requests to CA Swanson, Biostatistics Branch, Division of Cancer Etiology, NCI, NIH; 6130 Executive Blvd, EPN, Room 431; Rockville, MD 20892.

Received December 31, 1990.

Accepted for publication March 20, 1991.

TABLE 1
Subject characteristics

Characteristic	Subject					
		2	3	4	5	6
Age (y)	32	32	31	21	21	29
Sex	M	M	M	F	F	F
Weight (kg)	82.5	70.7	68.2	51.6	62.1	60.9
Height (m)	1.74	1.76	1.74	1.66	1.74	1.66
Quetelet index*	27.2	22.8	22.5	18.7	20.5	22.1
Plasma volume (L)†	3.7	3.2	3.1	2.3	2.8	2.7
Hematocrit	0.43	0.42	0.41	0.42	0.40	0.38
Plasma selenium ($\mu\text{mol/L}$)‡	1.61	2.09	1.89	1.80	1.72	1.51

* Calculated as kg/m^2 .

† Estimated at $0.045 \times$ subject weight (in kg).

‡ Average values of total plasma selenium for study days (excluding dose day).

After an overnight fast, subjects were given a single oral 200- μg dose of ^{74}Se as L-selenomethionine ($[^{74}\text{Se}]\text{SeMet}$) in distilled deionized water. The labeled SeMet was prepared commercially (Amersham Corp, Arlington Heights, IL) by using enriched ^{74}Se obtained as elemental selenium (Oak Ridge National Laboratory, Oak Ridge, TN).

Sample collection, preparation, and analysis

No detectable selenium was found in any of the materials used for collecting and measuring specimens. Precautions were taken against environmental selenium contamination, and blanks carried through collection procedures showed no evidence of such contamination. Detailed methods of sample collection are given elsewhere (10).

After the dose, blood was drawn at 30 min, 60 min, hourly for the next 7 h, daily for days 1–5 and 11, and then weekly for 2–3 wk. After dose day all samples were drawn while subjects were fasting. Two-hour urine collections were made for the first 8 h, then a single 4-h collection and a single 12-h collection were made. Twenty-four-hour collections were made for the next 11 d. Daily fecal samples were collected for 12 d beginning on dose day.

The amount of ^{74}Se tracer, unenriched (natural) selenium, and total selenium in the samples was determined by using an isotope-dilution technique combined with gas-chromatography-mass-spectrometry analysis. Methods of sample preparation, digestion, and analysis are described elsewhere (12). The detection limit of the method (defined as three times the SD of the analytical blank) was 6 pmol Se.

Reference samples from the National Institute of Standards and Technology (NIST, Gaithersburg, MD) were processed and analyzed in the same manner as experimental samples; selenium content was within the estimated uncertainty of the NIST certified values. Quality control was maintained by regular determinations of in-house reference pools of serum, whole blood, and urine. Agreement of duplicate readings of the in-house reference pools was within 2% for blood and urine and 6% for feces.

Kinetic modeling

Through use of compartmental-analysis techniques, a kinetic model for human SeMet metabolism was proposed to account

simultaneously for the plasma, urine, and fecal data. Simulation and testing of the compartmental models was carried out by using the SAAM/CONSAM simulator (13) on a VAX-8350 computer system (Digital Equipment, Maynard, MA). Starting with the selenite model developed by Patterson et al (10), several models were proposed to describe the data until one was developed that provided an adequate fit to all of the observed data with no systematic deviations. Initial estimates for the parameters were obtained from the selenite model and the literature or were based on physiological constraints. When the final model was developed, the parameters were adjusted individually for each subject by using nonlinear least-squares techniques to obtain a best fit of the data. Using the final compartmental model and the corresponding parameters for each subject, we calculated turnover time (TT), which is defined as the average amount of time the tracer spends in a compartment or group of compartments. The residence time (the total amount of time that material spends in a compartment) will exceed the turnover time if a fraction of the material passes through the compartment more than once. Turnover time is related to half-life ($t_{1/2}$) as follows: $t_{1/2} = (\ln 2)TT$, or, approximately, $t_{1/2} = (0.693) TT$.

Plasma ^{74}Se concentration was measured in nanograms per milliliter and then converted to fraction of dose per liter by dividing by 200 (the size of the dose in μg). Urine and fecal values, measured in micrograms, were also divided by 200 to give fraction of dose per sample. These calculations normalize the data for comparison with other studies.

Results

Starting with the selenite model as the a priori structure, a similar model was postulated for SeMet. The a priori structure was modified until it was consistent with the SeMet data. The modifications represent the minimum number of changes to the a priori structure that were compatible with the experimental data. We begin by describing the selenite model and then show the stepwise development of the SeMet model.

The a priori (selenite) model

Under experimental conditions that were nearly identical to the present study, Patterson et al (10) developed a model to

describe the kinetics of selenite metabolism in humans. This model, shown in Figure 1, describes absorption, distribution, and excretion of selenite within a metabolic system.

The dose of labeled selenite is introduced into the first part of a chain of compartments (G1, G2, and G3) representing the absorptive and distributive portion of the gastrointestinal tract. Selenium is absorbed into a compartment labeled ENT representing the intestinal cells or enterocytes. After a delay, material that is not absorbed appears in the feces. This delay probably represents time spent in the large intestine.

The absorbed material leaves the enterocyte by two pathways. The first pathway represents the earliest appearance of material in the peripheral circulation and is shown by an arrow from ENT to the first plasma component P1. This pathway denotes material present in the blood passing through the portal vein but not removed by the liver. The selenite model also allows for removal of a fraction of the portal material as it passes through the liver (first-pass effect) resulting in a delayed appearance in the plasma. This pathway is represented by the dashed arrow from ENT to the liver-pancreas subsystem (L/P).

The remainder of the absorbed dose follows another pathway from the enterocytes, to the second component of the plasma pool, represented in the model by P2. Material following this path passes through a compartment labeled HPL, which is pos-

TABLE 2
Cumulative fraction of excreted ^{74}Se in humans after 12 study days*

	Selenite †	SeMet
	% of dose	
Feces	18 ± 1	4 ±
Urine	17 ± 1	11 ±
Total	35 ± 2	15 ±

* $\bar{x} \pm \text{SE}$; $n = 6$.

† Data from reference 10.

tulated to represent either lymphatic flow from the enterocytes or another pool in the hepatopancreatic subsystem. The delay in the appearance of label in this plasma component is a result of the time the label takes to move through HPL. From the first two components of the plasma pool, the tracer can be excreted in the urine or it can move into the compartments that taken together represent the liver and pancreas.

After a delay, the material leaves L/P by two pathways. The first is through a compartment labeled BILE, which may include liver bile and pancreatic secretions. Material is returned via this pathway to the gut; this represents enterohepatic recirculation.

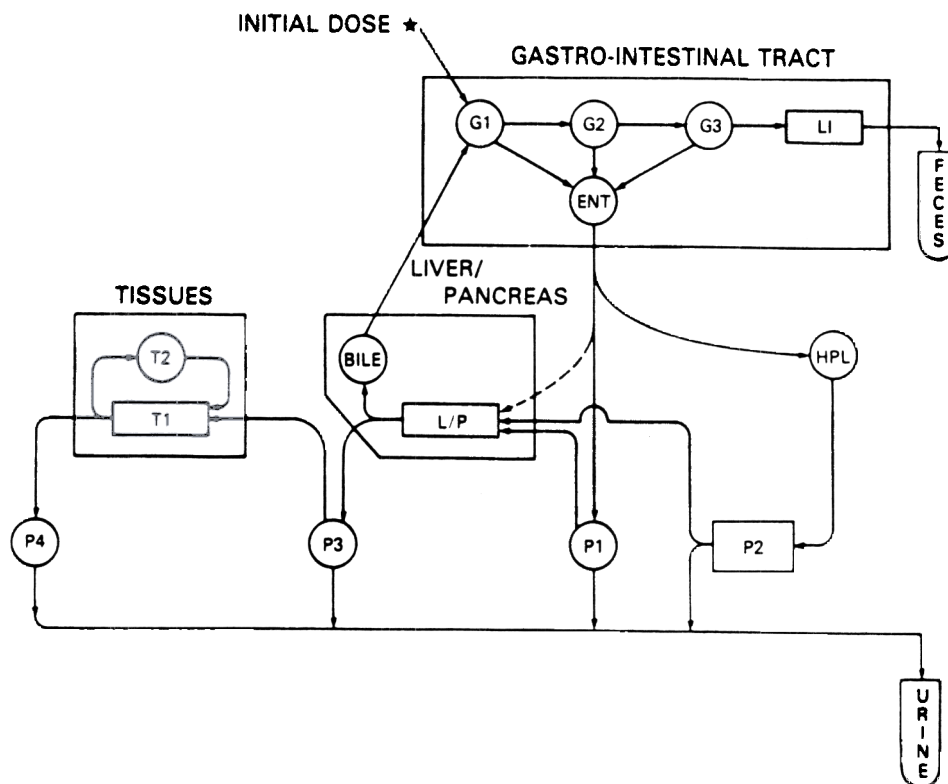


FIG 1. Selenite model, a kinetic model for selenite metabolism (10). The arrow with an asterisk indicates the site of entry of the oral tracer selenium. Arrows between compartments represent pathways of fractional transport. Compartments depicted as rectangles represent delays. G1, G2, G3, three gut compartments, probably small intestine; ENT, enterocytes (intestinal cells); HPL, compartment in hepatopancreatic subsystem or lymphatic system; L/P, liver and pancreas; LI, large intestine; T1, T2, peripheral tissues, in large part skeletal muscle. Feces and urine compartments are drawn in the shape of test tubes to represent fractional (single) collections. The model includes absorption distributed along the gastrointestinal tract, enterohepatic recirculation, four kinetically distinct plasma compartments P1-P4, a subsystem consisting of the liver and pancreas, and a tissue subsystem that is slowly turning over.

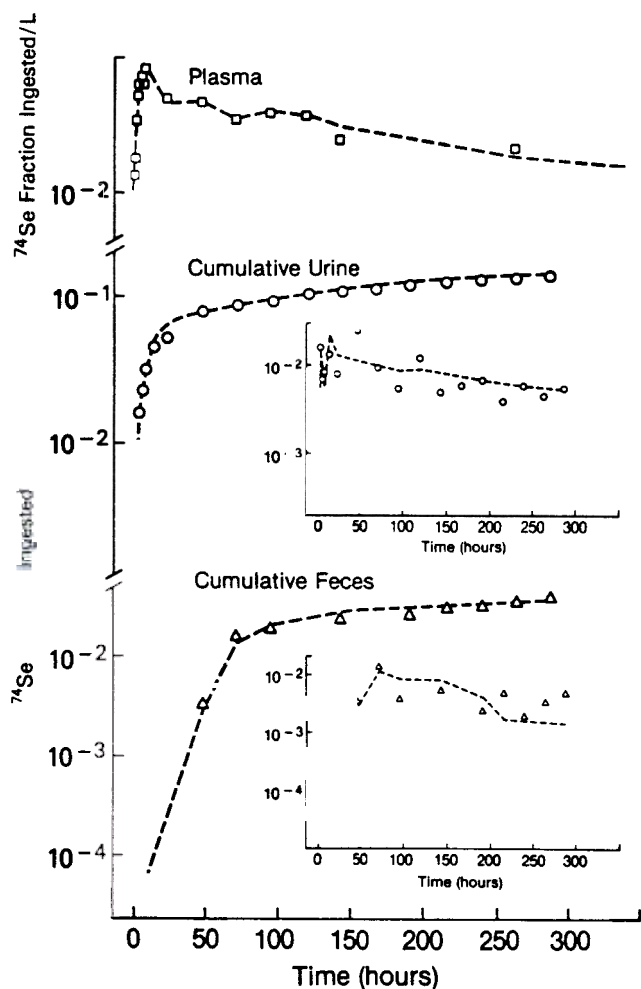


FIG 2. Plasma, urine, and fecal tracer data for subject 5 for the first 300 h after dosing. Cumulative urine and feces data represent the sum of the fractional data shown in the insets. Dashed lines indicate simultaneous fit of the observed plasma, urine, and fecal data using the SeMet model.

The second pathway leads to a third plasma component represented by P3. This component may represent proteins or selenoenzymes secreted or excreted by the liver or pancreas. From P3 the label can be excreted in the urine or can move into a subsystem labeled TISSUES.

The large tissue pool that turns over very slowly includes such peripheral tissues as the kidneys, muscle, and bone and is represented by two compartments that exchange with each other. Label flows from P3 to T1 and from T1 to P4, a fourth component of the plasma pool, and a tissue component, T2, in which label is sequestered. P4 is fed by the large tissue pool, and represents material emerging from the peripheral tissues through the plasma and being eliminated in the urine.

Development of the selenomethionine model

Before testing the SeMet data against the a priori selenite model, we compared the cumulative excretion of label from these two chemical forms of selenium (Table 2). After 12 collection days, subjects receiving [^{74}Se]SeMet excreted substantially less label in feces and in urine, indicating that the oral dose of

organically bound selenium was better absorbed and conserved than was the inorganic source. These important differences in selenium utilization were considered while developing the SeMet model.

Absorption. After parameter values were adjusted to reflect the increased absorption of [^{74}Se]SeMet, the a priori model provided an adequate fit to the fecal data. As shown in Figure 2, the first few fecal-data points were fit by a theoretical curve derived from a model in which the dose was introduced into a series of three compartments (G1, G2, and G3), each with an equal turnover time. The label continued to appear in the feces throughout the 12-d collection period, resulting in a positive slope of the tail of the cumulative fecal curve. The slope of the tail of this curve was consistent with a pathway for enterohepatic recirculation.

Distribution from enterocytes. The selenite model also adequately described the distribution of material from the enterocytes. The a priori model postulates that material is distributed from the enterocytes (ENT) to two kinetically distinct components (P1 and P2) of the plasma pool. Two peaks in the early plasma data and corresponding peaks in the fractional urine were consistent with two plasma components. The first plasma peak, which appeared as a shoulder on the early plasma curve of most subjects (Fig 3), was apparent for subjects 1, 2, and 4. Corresponding peaks were observed in the early fractional urine, as can be seen in data of a representative subject shown in Figure 2.

The selenite model allows for the possibility that a minor fraction of the material in the portal circulation is removed by the liver before appearing in the first plasma component (first-pass effect). The flow through this pathway was increased substantially to fit the SeMet data (Fig 4, B). Otherwise, the model predicted too much material in the early plasma (Fig 4, A).

Tissue distribution. About 15% of the administered [^{74}Se]SeMet dose was excreted during the first 12 d after dosing (Table 2). Only a small amount of the retained label was present in the plasma. This was determined by multiplying the peak plasma concentration of the label by the estimated plasma volume. The a priori model allowed for storage of material in peripheral tissues (T2), but even after material was sequestered in this tissue compartment, the model was not consistent with the data (Fig 5, A). First, the model predicted substantially more material in the plasma than was observed. Second, the observed data indicated that the tail of the plasma curve sloped gently downward whereas the curve predicted by the model was flat. Both discrepancies could be remedied by increasing the rate of elimination of material from the fourth plasma compartment (P4). Excess material in P4, however, could not be directed to the urine because the model already predicted slightly more material in the urine than was observed. To simultaneously account for the plasma and urine data, the model was modified by adding a pathway from P4 back to the liver. This modification allowed for reutilization of labeled material. The addition of this pathway improved the agreement between the model and the observed data (Fig 5, B) for all subjects.

A final inconsistency remained. The observed plasma data were not compatible with the single tissue pool as described in the a priori model; rather, they suggested two kinetically distinct peripheral tissue pools. The fit of the data was improved (Fig 5, C) by resolving into two subgroups peripheral tissues that are

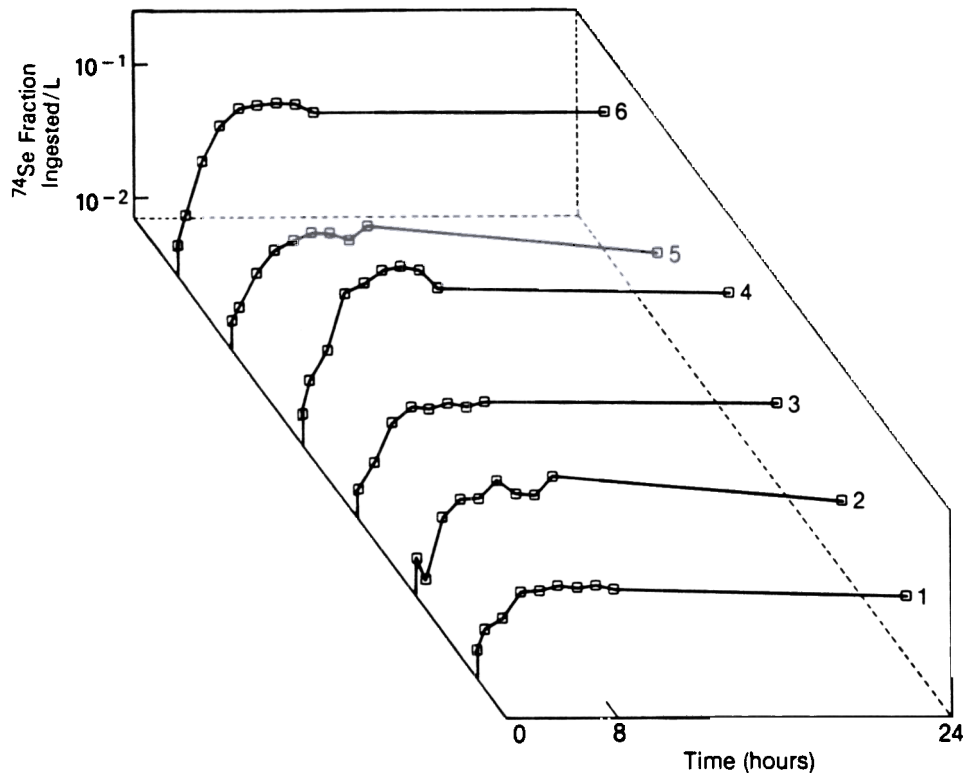


FIG 3. Plasma ^{74}Se data for the first 24 h after dosing. To illustrate patterns, observations for each subject were normalized to the 30-min sample and connected by lines without fitting. Numbers refer to subjects.

slowly turning over (Tissues A and B), each subgroup having different turnover times.

Selenomethionine model

The SeMet model is shown in Figure 6. Modifications to the a priori selenite model are indicated by heavy solid lines. First, $[^{74}\text{Se}]\text{SeMet}$ was absorbed more completely than was $[^{74}\text{Se}]\text{selenite}$. Second, a path to L/P from ENT was needed to fit the SeMet data whereas the first-pass effect was insignificant in the selenite model. Third, the SeMet data were consistent with a model in which material from the peripheral tissues traveled through the plasma and then back to the liver. The selenite model did not contain a pathway for conservation of selenium metabolites from these tissues. Fourth, the SeMet data were consistent with two kinetically distinct peripheral tissue pools; the selenite model required only a single pool.

The parameters derived from the SeMet model are shown in Table 3. They describe the absorption, distribution, and excretion of $[^{74}\text{Se}]\text{SeMet}$. Individual data are presented because of the small sample size. After accounting for enterohepatic recirculation, the absorption of label from SeMet was 98%. SeMet leaving the enterocytes was partitioned among L/P (53%), P1 (30%), and P2 (17%). Most of the material moving from ENT to P1 and P2 returned to the liver; at most, 14% was excreted in the urine. Material leaving the liver was partitioned between a pathway back to the gastrointestinal tract (46%) and a pathway to P3. Only a small fraction of label in P3 (~3%) was excreted in urine. Most of the material leaving P3 was delivered to the peripheral tissues. Not all of this material was stored. Of the material from P3 delivered to Tissues A, ~65% returned to the plasma after

a delay of 29 h. After a delay of 140 h, ~35% of material in Tissues B returned to the plasma. Label from the tissues was transported to the peripheral circulation (P4) and only 5% was excreted in the urine. Most of the material leaving P4 returned to the liver.

Turnover times are shown in Table 4. Average turnover times for the four plasma components varied from 0.01 to 1.1 d for the six subjects. The turnover time in the liver and pancreas ranged from 1.6 to 3.1 d. Turnover times were longer in the peripheral tissues, ranging from 16 to 27 d for Tissues A and from 61 to 86 d for Tissues B. The whole-body residence time was approximately five-fold greater than the turnover time of the slowest turning-over tissue pool, reflecting substantial reutilization of material. In the absence of reutilization, the whole-body residence time would be expected to be less than the turnover time of the slowest component in the system.

Discussion

One means of examining the model is to determine whether our representation of SeMet utilization is compatible with existing knowledge. Additionally we can compare SeMet utilization in the present study and selenite utilization in our earlier study. Differences in the utilization of Se from the two chemical forms are recognized (11), and our comparison should reflect those differences.

Plasma pool

The plasma curves (Fig 3) of the present study are remarkably similar to those observed in our companion selenite study (10).

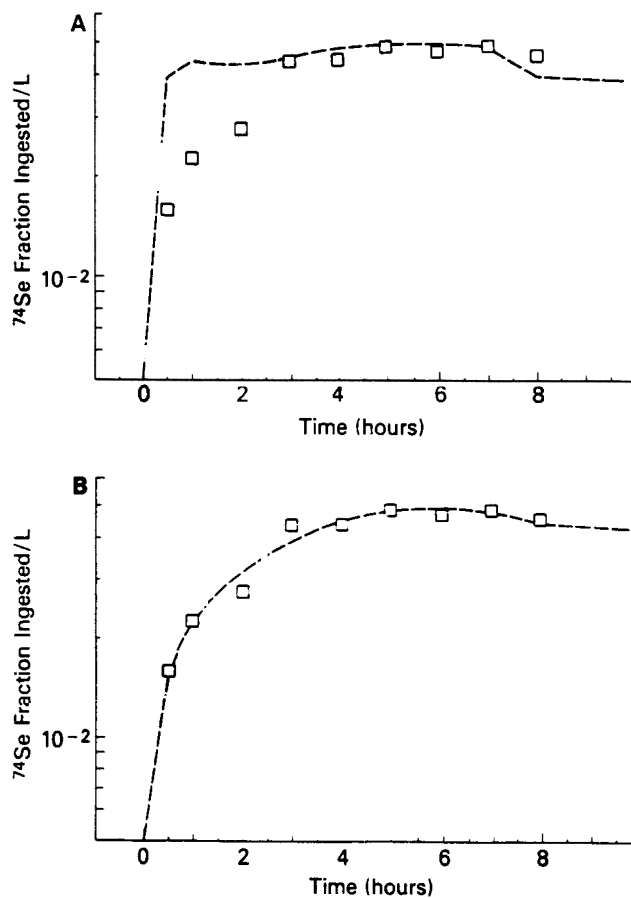


FIG 4. Theoretical plasma curve for subject 1 before (A) and after (B) adjustment of the parameters describing the first-pass effect.

The similarity was unexpected given that selenomethionine and selenite are so dissimilar chemically. Although the plasma curves in both studies were resolved into the same number of components, we do not infer from the model structures that the two chemical forms of selenium have the same metabolic fate. Indeed, simultaneous accounting of label in plasma, urine, and feces indicated many differences in the movement and disposition of label from the two sources.

Absorption

Other studies indicate that SeMet is better absorbed than selenite (7, 14, 15). For example, two New Zealand women of low selenium status (7, 15) absorbed 44–70% of selenium from selenite and 96% of selenium from SeMet. In our studies, absorption of ^{74}Se from selenite was 84% compared with 98% for SeMet.

Distribution from enterocytes

In the present study our model suggests a pronounced first-pass effect. In our companion selenite study (10), by contrast, most of the selenium in the portal circulation was not initially removed by the liver but rather was first distributed to P1. Griffiths et al (7) also concluded that liver uptake of selenium is more rapid after a dose of organically bound selenium than after a dose of inorganic selenium.

Liver-pancreas subsystem

Labeled material appeared in the third component of the plasma pool 7–8 h after dosing and peaked at ~ 10 h. The same

plasma component was observed in the selenite study (10) and a similar peak was also noted in two other tracer studies in humans (15, 16). The material in this component is probably a protein or selenoenzyme produced by the liver.

Material in P3 was transported to the peripheral tissues with only a small fraction excreted in the urine. Less than 3% of the label in P3 was excreted in the urine compared with 11% of the material in P1. Others reported that the fraction of ingested selenium excreted in urine decreases with time (17). As suggested

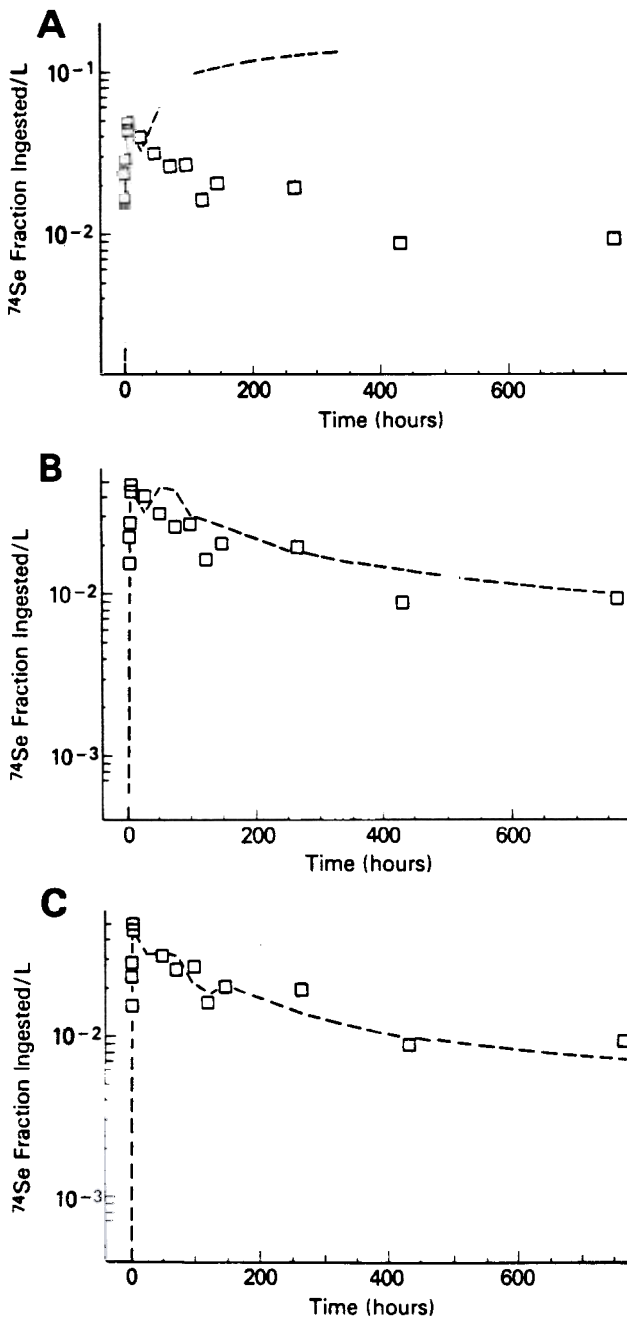


FIG 5. Theoretical plasma curve for subject 1 before (A) and after (B and C) changing the model structure. B: Fit of the model to the data after adding a pathway for reutilization of selenium metabolites from peripheral tissues. C: Fit of the model to the data after adding a second peripheral tissue pool.

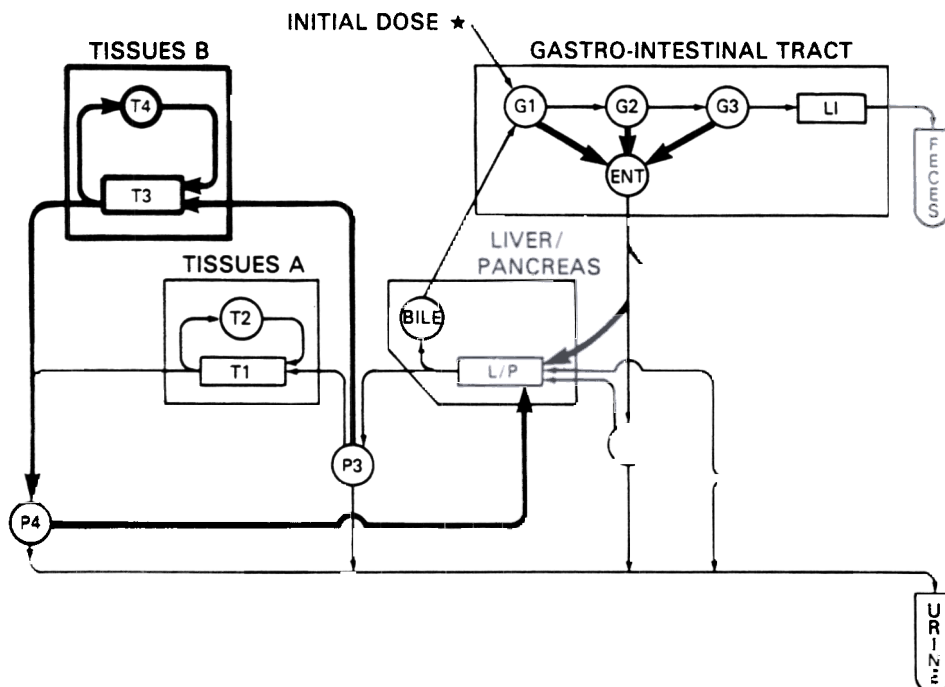


FIG 6. Selenomethionine model, a kinetic model for $[^{74}\text{Se}]\text{SeMet}$ metabolism. The arrow with an asterisk indicates the site of entry of the oral tracer selenium. Arrows between compartments represent pathways of fractional transport. Compartments depicted as rectangles represent delays. G1, G2, and G3, three gut compartments, probably small intestine: ENT, enterocytes (intestinal cells); HPL, compartment in hepatopancreatic subsystem or lymphatic system; L/P, liver and pancreas; LI, large intestine; T1, T2, T3, T4, peripheral tissues, eg, skeletal muscle, bone, kidney. Feces and urine compartments are drawn in the shape of test tubes to represent fractional (single) collections. The model includes absorption distributed along the gastrointestinal tract, enterohepatic recirculation, four kinetically distinct plasma compartments P1-P4, a subsystem consisting of the liver and pancreas, two tissue subsystems that are slowly turning over, and a pathway for reutilization of selenium metabolites from peripheral tissues. The heavy solid lines indicate the major modifications to the a priori selenite model (Fig 1).

by Robinson et al (18), the earliest peak of selenium in urine probably represents material that is absorbed but not utilized whereas later peaks represent loosely bound or bound selenium.

In our models some of the label in L/P was returned to the gastrointestinal tract. Only small amounts of selenium were found in rat bile (19), but Charlesworth et al (20) noted a high concentration of radioactivity in the bile of humans injected with $[^{75}\text{Se}]\text{SeMet}$. The pancreas has such a high affinity for selenium from organically bound sources that $[^{75}\text{Se}]\text{SeMet}$ is used clinically as a scanning agent (21). Presumably, selenium would be present in pancreatic secretions.

Peripheral tissues

The plasma component P4 represents labeled material emerging from tissues such as muscle, bone, kidney, and other organs. Resolution of peripheral tissues into more than a single pool was reasonable given that this subsystem is heterogeneous and includes not only different organs but also different tissues and cell types.

The whole-body turnover time of selenium is determined largely by the peripheral tissues. These tissues contain skeletal muscle and contribute ~60% to the total body selenium content (11). Several investigators estimated $[^{75}\text{Se}]\text{SeMet}$ turnover in peripheral tissues by examining the slowest exponential component of whole-body ^{75}Se decay curves. Ben-Porath et al (5) determined

an average turnover of 130 d in nine healthy subjects receiving an intravenous dose of $[^{75}\text{Se}]\text{SeMet}$. Lathrop et al (6) calculated a value of 220 d. A report by New Zealand investigators (7) is of particular interest because the whole-body turnover of $[^{75}\text{Se}]\text{SeMet}$ was about two times longer than that of $[^{75}\text{Se}]\text{selenite}$. In our studies, ^{74}Se from SeMet also stayed in the body more than twice as long as ^{74}Se from selenite (Table 5). However, we do not attribute this difference to slower peripheral tissue turnover of ^{74}Se from SeMet . On the contrary, the turnover of ^{74}Se in plasma, liver, and tissues was more rapid for $[^{74}\text{Se}]\text{SeMet}$ than for $[^{74}\text{Se}]\text{selenite}$. We attribute the slower whole-body turnover of $[^{74}\text{Se}]\text{SeMet}$ to reutilization.

Reutilization marks one of the most dramatic differences between SeMet and selenite utilization. Other studies also suggest that SeMet is reutilized. Awwad et al (22) monitored the appearance of radioactivity in hemoglobin of rats given an injection of labeled plasma protein obtained from donor animals injected with $[^{75}\text{Se}]\text{SeMet}$. The plasma label was incorporated efficiently into hemoglobin. Data from humans also indicate considerable recycling of organically bound Se. In two studies significant amounts of labeled selenium were obtained from erythrocytes collected 35-52 wk after dosing (7, 23); the lifespan of red blood cells is < 130 d. Twenty years ago two groups concluded that $[^{75}\text{Se}]\text{SeMet}$ could not be used as an indicator of whole-body protein turnover because SeMet was so extensively reutilized

TABLE 3
Parameters derived from selenomethionine model*

	Subject						$\bar{x} \pm SE$
	2	3	4	5	6		
Absorption and fecal excretion							
L [ENT, G1] (h^{-1})	0.900	0.902	0.850	0.504	1.29	0.830	0.879 \pm 0.102
L [ENT, G2] (h^{-1})	1.02	0.935	0.860	0.522	1.20	0.900	0.906 \pm 0.091
L [ENT, G3] (h^{-1})	0.020	0.022	0.020	0.012	0.030	0.020	0.021 \pm 0.002
Fraction absorbed	0.963	0.974	0.979	0.979	0.973	0.983	0.975 \pm 0.003
L [G2, G1] (h^{-1})	0.300	0.198	0.150	0.096	0.210	0.170	0.187 \pm 0.028
L [G3, G2] (h^{-1})	0.180	0.165	0.140	0.078	0.300	0.100	0.160 \pm 0.032
Delay in G1, G2, G3 (h)	0.830	0.909	1.00	1.67	0.666	1.00	1.01 \pm 0.14
L [LI, G3] (h^{-1})	0.045	0.050	0.045	0.052	0.050	0.050	0.049 \pm 0.001
Delay in LI (h)	8.1	5.2	4.1	7.2	35.2	10.2	11.7 \pm 4.8
Urinary excretion							
L [urine, P1] (h^{-1})	0.18	0.45	0.60	0.90	0.75	0.75	0.60 \pm 0.10
Fraction to urine from P2	0.085	0.000	0.145	0.091	0.133	0.038	0.082 \pm 0.023
L [urine, P3] (d^{-1})	0.001	0.006	0.001	0.001	0.003	0.001	0.002 \pm 0.001
L [urine, P4] (d^{-1})	0.003	0.001	0.002	0.002	0.002	0.002	0.002 \pm 0.000
Distribution from enterocyte							
Delay in ENT (h)	0.036	0.037	0.038	0.037	0.036	0.037	0.037 \pm 0.000
L [L/P, ENT] (h^{-1})	13.6	13.1	13.2	17.0	15.8	13.6	14.4 \pm 0.7
L [P1, ENT] (h^{-1})	9.0	9.5	8.8	5.6	6.8	9.0	8.1 \pm 0.6
L [HPL, ENT] (h^{-1})	5.5	4.2	4.0	4.7	5.0	4.5	4.6 \pm 0.2
Fraction to L/P	0.482	0.489	0.508	0.621	0.573	0.500	0.529 \pm 0.022
Fraction to P1	0.322	0.354	0.338	0.207	0.247	0.334	0.303 \pm 0.024
Fraction to HPL	0.196	0.157	0.154	0.172	0.181	0.166	0.171 \pm 0.006
Liver-pancreas subsystem							
L [L/P, P1] (h^{-1})	2.65	4.55	4.40	6.50	4.45	6.25	4.80 \pm 0.58
Fraction to L/P from P1	0.936	0.910	0.880	0.878	0.856	0.893	0.892 \pm 0.011
L [P2, HPL] (h^{-1})	0.90	1.10	0.60	0.45	0.70	0.70	0.74 \pm 0.09
Delay in P2	6.3	5.7	5.3	5.6	6.0	5.2	5.7 \pm 0.2
Fraction to L/P from P2	0.914	1.00	0.855	0.909	0.867	0.962	0.92 \pm 0.02
Minimum delay in L/P (h)	7.6	7.4	7.5	8.0	7.4	7.7	7.6 \pm 0.1
Fraction to P3	0.55	0.065	0.45	0.50	0.50	0.60	0.54 \pm 0.03
L [P3, L/P] (h^{-1})	4.4	5.2	3.6	4.0	4.0	4.8	4.3 \pm 0.2
Fraction to bile	0.45	0.35	0.55	0.50	0.50	0.40	0.46 \pm 0.03
L [BILE, L/P] (h^{-1})	3.6	2.8	4.4	4.0	4.0	3.2	3.7 \pm 0.2
L (G1, BILE) (d^{-1})	0.012	0.006	0.013	0.016	0.008	0.006	0.010 \pm 0.002
L [L/P, P4] (h^{-1})	0.045	0.024	0.042	0.040	0.027	0.047	0.038 \pm 0.004
Tissues							
Tissues A							
L [T1, P3] (h^{-1})	0.083	0.056	0.055	0.096	0.055	0.077	0.070 \pm 0.007
Minimum delay (h)	29.0	31.0	30.0	30.0	19.0	34.0	28.8 \pm 2.1
Fraction stored	0.393	0.300	0.308	0.444	0.377	0.333	0.359 \pm 0.020
L [T1, T2] (h^{-1})	0.0016	0.0007	0.0007	0.0020	0.0010	0.0015	0.0012 \pm 0.0002
Tissues B							
L [T3, P3] (h^{-1})	0.038	0.063	0.035	0.083	0.051	0.044	0.052 \pm 0.007
Minimum delay (h)	130	140	160	170	78	160	140 \pm 14
Fraction stored	0.666	0.750	0.600	0.588	0.666	0.600	0.645 \pm 0.025
L [T3, T4] (h^{-1})	0.0015	0.0025	0.0012	0.0010	0.0011	0.0014	0.0014 \pm 0.0002

* L (I, J), fractional rate of flow from compartment J to compartment I; ENT, enterocyte; LI, large intestine; HPL, hepatopancreatic or lymphatic compartment; L/P, liver and pancreas; P1-P4, plasma compartments; G1-G3, gut compartments; T1-T4, peripheral-tissue compartments.

(24, 25). This phenomenon could be biologically advantageous if recycled material were incorporated into physiologically active species. An investigation conducted in Finland indicates that this does occur (26). Men of low selenium status were supplemented for 11 wk with selenate, selenium-rich wheat, or selenium-rich yeast. Ten weeks after the supplement was discontinued, glutathione peroxidase activity remained elevated in individuals who had received the organically bound selenium.

As noted above, the turnover of labeled selenium in various compartments was more rapid for [^{74}Se]SeMet than for [^{74}Se]selenite. It is widely assumed that SeMet turns over more slowly than does selenite because inorganic selenium cannot be incorporated into general body proteins (11). Slow turnover of selenium from SeMet has been used to explain the observation of higher tissue selenium concentrations of animals fed SeMet when compared with animals fed selenite. Our models indicate

TABLE 4
[⁷⁴Se] SeMet turnover time of adults given a single oral 200- μ g dose of isotope

	2	3	4	5	6	$\bar{x} \pm SE$	
	<i>d</i>						
Plasma, average	0.51	0.84	0.55	0.52	0.74	0.52	0.61 \pm 0.06
P1	0.01	0.01	0.01	0.01	0.01	0.01	0.01 \pm 0.00
P2	0.26	0.24	0.22	0.23	0.25	0.22	0.24 \pm 0.01
P3	0.34	0.33	0.46	0.23	0.38	0.34	0.35 \pm 0.03
P4	0.88	1.8	0.95	0.99	1.4	0.84	1.1 \pm 0.2
Liver/pancreas	1.9	2.7	2.1	1.6	3.1	3.1	2.4 \pm 0.3
Peripheral tissues							
Tissues A	19	27	27	19	26	16	22 \pm 2
Tissues B	72	73	69	77	86	61	73 \pm 3
Whole body	309	397	329	416	310	416	363 \pm 21

that label from SeMet turns over in individual compartments more rapidly than does label from selenite. Therefore, tissue accumulation must be a result of extensive recycling of SeMet.

Limitations of the model

A fundamental assumption of steady-state kinetics is that the amount of tracer is so small as to not disturb the dynamic state of the underlying system. In weanling rats whole-body retention of injected [⁷⁵Se]selenite was influenced by large carrier doses (27). In the present study the tracer dose exceeded the usual intake of the subjects but, relative to body weight, was considerably smaller than the tracer dose used in the animal study. If the tracer dose perturbed the system, the fractional rate constants could be somewhat smaller or larger than if the system had been studied in a true steady state but the structure of the model would probably not be affected.

Parameter estimates and turnover calculations would be affected by failure to measure all routes of selenium elimination. Lathrop et al (28) measured ⁷⁵Se in hair, nails, and skin of one subject injected with [⁷⁵Se]SeMet. During the first 280 d, only 4% of the injected label was eliminated through these tissues. Loss of selenium in expired air is negligible when selenium intake is within the nutritional range (15, 28).

We studied the utilization of a specific chemical form of selenium in subjects of adequate selenium status. Neither the parameters nor the structure of this model can be assumed to hold across all levels of selenium intake. Finally, although it is widely

assumed that SeMet is the predominant chemical form of selenium in foods, data are limited. Until the chemical forms of selenium in food are characterized, it should not be assumed that data from this study are representative of all food selenium.

In summary, SeMet was rapidly and completely absorbed. Selenium from SeMet was better absorbed and retained than selenium from selenite. The slower whole-body turnover of SeMet was attributed to efficient reutilization as opposed to slow turnover of label incorporated into general body proteins. If recycled material is incorporated into metabolically active species, reutilization of selenium from SeMet could be physiologically advantageous. At high intakes, however, reutilization of selenium from SeMet could result in excessive tissue accumulation and toxicity. \square

References

1. Keshan Disease Research Group, Chinese Academy of Medical Sciences. Observations on effect of sodium selenite in prevention of Keshan disease. *Chin Med J* 1979;92:471-6.
2. Salonen JT, Alfthan G, Huttunen JK, Pikkariainen J, Puska P. Association between cardiovascular death and myocardial infarction and serum selenium in a matched-pair longitudinal study. *Lancet* 1982;2:175-9.
3. Varo P, Alfthan G, Ekholm P, Aro A, Koivistoinen P. Selenium intake and serum selenium in Finland: effects of soil fertilization with selenium. *Am J Clin Nutr* 1988;48:324-9.
4. Willett WC, Stampfer MJ. Selenium and cancer. *Br Med J* 1988;297:573-4.
5. Ben-Porath M, Case L, Kaplan E. The biological half-life of ⁷⁵Se-selenomethionine in man. *J Nucl Med* 1968;9:168-9.
6. Lathrop KA, Johnston RE, Blau M, Rothschild EO. Radiation dose to humans from ⁷⁵Se-L-selenomethionine. *J Nucl Med* 1972;13(suppl):9-30.
7. Griffiths NM, Stewart RDH, Robinson MF. The metabolism of [⁷⁵Se]selenomethionine in four women. *Br J Nutr* 1976;35:373-82.
8. Krishnamurti CR, Ramberg CF Jr, Shariff MA. Kinetic modeling of selenium metabolism in nonpregnant ewes. *J Nutr* 1989;119:1146-55.
9. Janghorbani M, Christensen MJ, Nahapetian A, Young VR. Dynamics of selenite metabolism in young men: studies with the stable isotope tracer method. *Am J Clin Nutr* 1984;40:208-18.
10. Patterson BH, Levander OA, Helzlsouer K, et al. Human selenium metabolism: a kinetic model. *Am J Physiol* 1989;257(Regulatory Integrative Comp Physiol 26):R556-67.

TABLE 5
Comparison of ⁷⁴Se turnover, from labeled SeMet and selenite*

	Selenite†	SeMet
	<i>d</i>	
Plasma	2.0 \pm 0.1	0.6 \pm 0.1
Liver and pancreas	20 \pm 5	2.4 \pm 0.3
Tissues	221 \pm 33	73 \pm 3
Whole-body	147 \pm 13	363 \pm 21

* $\bar{x} \pm SE$; $n = 6$.

† Data from reference 10.

11. International Programme on Chemical Safety. Environmental health criteria 58: selenium. Geneva: World Health Organization, 1987.
12. Reamer DC, Veillon C. A double isotope dilution method for using stable isotopes in metabolic tracer studies: analysis by gas chromatography/mass spectrometry (GC/MS). *J Nutr* 1983;113:786-92.
13. Berman M, Weiss MF. SAAM manual 1978. Washington, DC: US Government Printing Office, 1978. [DHEW publication (NIH) 76-730.]
14. Thomson CD, Stewart RDH. Metabolic studies of [⁷⁵Se]selenomethionine and [⁷⁵Se]selenite in the rat. *Br J Nutr* 1973;30:139-47.
15. Thomson CD, Stewart RDH. The metabolism of (⁷⁵Se) selenite in young women. *Br J Nutr* 1974;32:47-57.
16. Janghorbani M, Christensen MJ, Nahapetian A, Young VR. Selenium metabolism in healthy adults: quantitative aspects using the stable isotope ⁷⁴SeO₂³⁻. *Am J Clin Nutr* 1982;35:647-54.
17. Thomson CD, Burton CE, Robinson MF. On supplementing the selenium intake of New Zealanders. I. Short experiments with large doses of selenite or selenomethionine. *Br J Nutr* 1978;39:579-87.
18. Robinson MF, Rea HM, Friend GM, Stewart RDH, Snow PC, Thomson CD. On supplementing the selenium intake of New Zealanders. 2. Prolonged metabolic experiments with daily supplements of selenomethionine, selenite and fish. *Br J Nutr* 1978;39:589-600.
19. Levander OA, Baumann CA. Selenium metabolism vs. effect of arsenic on the excretion of selenium in the bile. *Toxicol Appl Pharmacol* 1966;9:106-15.
20. Charlesworth D, Pullan BR, Torrance B. Radio-isotope scanning in the diagnosis of pancreatic disease. *Br J Surg* 1970;57:413-7.
21. Blau M, Bender MA. Se⁷⁵-selenomethionine for visualization of the pancreas by isotope scanning. *Radiology* 1962;78:974.
22. Awwad HK, Adelstein J, Potchen EJ, Dealy JB Jr. The interconversion and reutilization of injected ⁷⁵Se-selenomethionine in the rat. *J Biol Chem* 1967;242:492-500.
23. Veillon C, Patterson KY, Button LN, Sytkowski AJ. Selenium utilization in humans—a long-term, self-labeling experiment with stable isotopes. *Am J Clin Nutr* 1990;52:155-8.
24. Waterlow JC, Garrow JS, Millward DJ. The turnover of [⁷⁵Se] selenomethionine in infants and rats measured in a whole body counter. *Clin Sci* 1969;36:489-504.
25. Said AK, Hegsted DM. ⁷⁵Se-selenomethionine in the study of protein and amino acid metabolism of adult rats. *Proc Soc Exp Biol Med* 1970;133:1388-91.
26. Levander OA, Alfthan G, Arvilommi H, et al. Bioavailability of selenium to Finnish men as assessed by platelet glutathione peroxidase activity and other blood parameters. *Am J Clin Nutr* 1983;37:887-97.
27. Burk RF, Brown DG, Seely RJ, Scaief CC. Influence of dietary and injected selenium on whole-body retention, route of excretion, and tissue retention of ⁷⁵SeO₃²⁻ in the rat. *J Nutr* 1972;102:1049-56.
28. Lathrop KA, Harper PV, Malkinson FD. Human total-body retention and excretory routes of ⁷⁵Se from selenomethionine. In: Fellinger K, Hofer R, eds. Radioactive isotopes in the clinic and research. Munich, FRG: Urban and Schwarzenberg, 1968:436-43.